Improved sensing using simultaneous deep UV Raman and fluorescence detection

R. Bhartia*[a], W. F. Hug[b], and R.D. Reid[b],
[a] Jet Propulsion Laboratory/Caltech, 4800 Oak Grove Dr., Pasadena, CA 91109
[b] Photon Systems, Inc., 1512 Industrial Park St., Covina, CA 91722

Abstract

Photon Systems in collaboration with JPL are continuing development of a new technology robot-mounted or hand-held sensor for reagentless, short-range, standoff detection and identification of trace levels chemical, biological, and explosive (CBE) materials on surfaces. This deep ultraviolet CBE sensor is the result of ongoing Army STTR and DTRA programs. The evolving 15 lb, 20 W, lantern-size sensor can discriminate CBE from background clutter materials using a fusion of deep UV excited resonance Raman (RR) and laser induced native fluorescence (LINF) emissions collected is less than 1 ms. RR is a method that provides information about molecular bonds, while LINF spectroscopy is a much more sensitive method that provides information regarding the electronic configuration of target molecules.

Standoff excitation of suspicious packages, vehicles, persons, and other objects that may contain hazardous materials is accomplished using excitation in the deep UV where there are four main advantages compared to near-UV, visible or near-IR counterparts. 1) Excited between 220 and 250 nm, Raman emission occur within a fluorescence-free region of the spectrum, eliminating obscuration of weak Raman signals by fluorescence from target or surrounding materials. 2) Because Raman and fluorescence occupy separate spectral regions, detection can be done simultaneously, providing a much wider set of information about a target. 3) Rayleigh law and resonance effects increase Raman signal strength and sensitivity of detection. 4) Penetration depth into target in the deep UV is short, providing separation of a target material from its background or substrate.

Keywords: deep UV Raman & native fluorescence; chemical, biological, and explosives detection and classification

1. INTRODUCTION

The ability to detect trace levels of chemical, biological, and explosive (CBE) materials on surfaces with a single, reagentless, hand-held or robot-mounted standoff sensor represents a major improvement in the state of the art of CBE surface sensors. We report here on the status of development of these sensors which can detect and identify less than 1 $\mu g/cm^2$ of explosives or 10^4 bacterial spores at 10 meters standoff, or 10 ng/cm^2 of explosives or 10^2 bacterial $spores/cm^2$ at 1 meter standoff. The sensor detects and identifies materials on surfaces in less than 1 ms and has a sample rate up to 20 Hz.

The new sensor, nominally called a targeted ultraviolet chemical, biological, and explosives (TUCBE) sensor, is the subject of this paper. This new sensor is designed for operation on small military robots, such as the iRobot PackBot EOD, or Foster-Miller Talon, or as a hand-held sensor. The present TUCBE sensor is nominally 15 lbs in weight and consumes less than 20 W from a battery or robot power source. Similar sensors with the same key components have been rated independently by the U.S. Army and NASA at technical readiness level (TRL) of 5.0+ in 2006. Versions of this sensor have been deployed on many expeditions to Antarctica, the Arctic, and the deep Ocean. This sensor uses a combination of resonance Raman (RR) and laser induced native fluorescence (LINF) spectroscopic methods with lasers emitting at either 224.3 nm or 248.6 nm.

2. DEEP UV RAMAN AND LASER INDUCED NATIVE FLUORESCENCE

A broad perspective of the relationship between Raman and native fluorescence spectral regions is illustrated below in Fig. 1 along with the emission wavelength of typical lasers and the spectral range of their Raman range. It is commonly accepted practice to move to the near IR to avoid fluorescence from target molecules or surrounding materials within the exposure volume, but with excitation even as high as 830 nm, it has been shown that a large fraction of materials

investigated exhibit major fluorescence interference[1] to the point that it completely obscures Raman emissions. Asher[2],[3] showed that natural materials did not fluoresce below a wavelength about 270nm, independent of the excitation wavelength. This was further proven in many subsequent publications such as Nelson[4], Sparrow[5], Wu[6], and many others. When excitation occurs below about 250nm, a fluorescence-free region exists above the laser wavelength in which to observe Raman spectra. This is not the case for lasers that provide excitation at longer wavelengths.

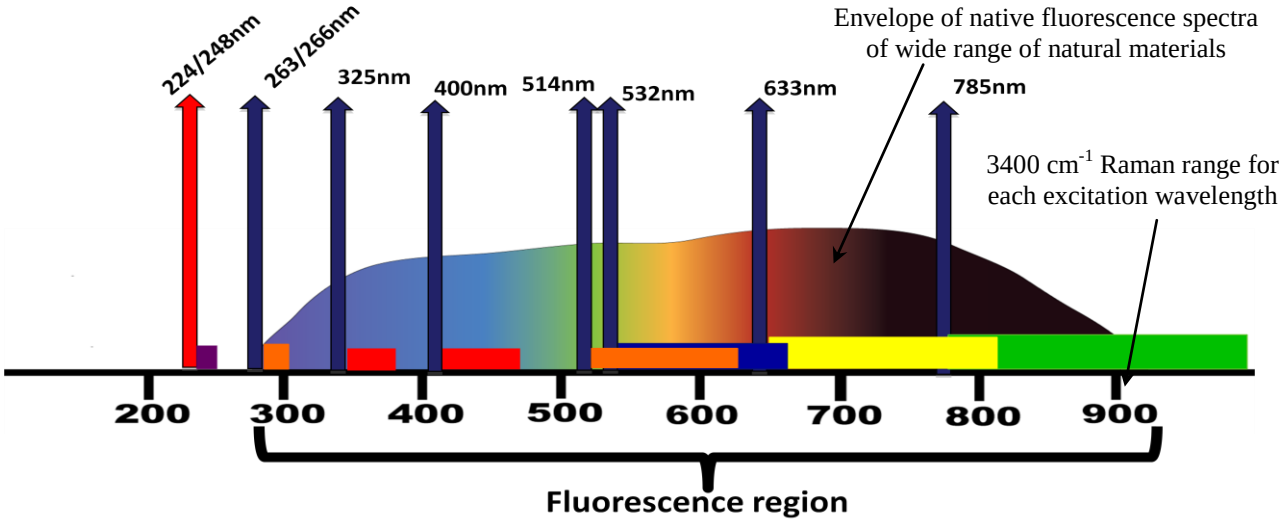

Figure 1. Broad relationship between Raman and native fluorescence spectral regions with emission wavelengths of typical lasers and their 4000 cm^{-1} Raman range.

Deep UV optical sensors for detecting and classifying or identifying CBE materials UV have several advantages over sensor operating in the near-UV, visible, or near-IR. These advantages are summarized as:

1. Clear Raman spectra with no obscuration of weak Raman spectra by native fluorescence or alteration of the fluorescence spectra by major C-H and O-H Raman bands. Raman and fluorescence are truly independent and orthogonal measurements.
2. The ability to simultaneously detect Raman and native fluorescence emissions from target materials with no possible confusion due to overlapping spectra regions.
3. Much higher sensitivity due to Rayleigh law and resonance Raman signal enhancements, providing much lower limits of detection of CBE agents
4. Simplification of Raman spectra due to resonance effects, enabling the use of Raman marker bands in the chemometric method
5. Short depth of penetration into target materials allowing discrimination against background materials.
6. Solar blind detection of Raman and fluorescence because of short operating wavelength, and gated detection
7. Non-contact, non-destructive, no sample handling
8. Reagentless
9. Reduced eye hazard (DHHS/CDRH Class I based on single data sample, Class IIIb based on repetitive sampling)
10. Longer depth of focus without the need to focus the sensor

3. THE FUSED RAMAN AND FLUORESCENCE SENSOR METHOD

The TUCBE sensor method begins by firing a low energy pulse of deep UV laser light onto an unknown target. The laser pulse is about 100 mW at 248 nm for a duration less than 100 us, putting the TUCBE sensor into a DHHS/CDRH Class I category based on a single or up to about 10 laser pulses. For continuous pulsing the laser is Class IIIb. The laser energy is scattered and absorbed in the target material, generating Rayleigh and Raman scattering and fluorescence and phosphorescence emissions. These emissions are collected in a 180 degree backscatter optical system which includes the laser with beam expander, excitation injection optics, variable-focus telescope reflective objective mirror

system, dichroic separation of Rayleigh, Raman and fluorescence spectral regions, and individual spectrographs and detector arrays for the Raman and fluorescence emissions.

Rayleigh scattering is typically a very efficient process and provides some data about the absorbance or reflectivity of the target, although this information content is very limited. Raman scattering is a weak phenomenon which provides information about the presence or absence of specific molecular bonds and functional groups within the target material. Raman information is essential for targets which do not fluoresce such as aliphatics and simple compounds and compounds which are not distinguishable from matrix materials. Fluorescence and phosphorescence is at least 5 to 10 orders of magnitude more efficient than Raman scattering and provides information about the electronic structure and molecular complexity of the target material. All of this data is collected during each laser pulse with a duration less than 100 μs. The data are separately processed in integrated into a fused Raman and fluorescence chemometric method to provide a description of the chemical nature of the target.

An illustration of the importance of combing or fusing Raman and fluorescence information from targets is shown below in Fig. 2. Next to Rayleigh scattering, which contains relatively little information about a target, fluorescence and phosphorescence are the most efficient emitters from most target materials, providing the ability to detect and differentiate materials at much longer standoff distances and lower concentrations than Raman emissions. However, not all materials fluoresce or phosphoresce very well. It is a common misconception that fluorescence is not a very informative method since the fluorescence from different material cannot be distinguished, however as demonstrated in 2006 - 2008, excitation in the deep UV provides a unique differentiability [8-9]. Because of the efficiency of fluorescence from either target materials or their substrate or surrounding materials, weak Raman emissions are often masked unless excitation occurs below 250 nm. Separation of Raman and fluorescence emissions bands is essential even for weakly fluorescent materials or substrates. It is conversely true that strong water or CH Raman bands can also alter fluorescent emission spectra to lead to inaccurate conclusions unless these two spectral regions are separated. Materials that exhibit detectable Raman and fluorescence emissions include ammonium nitrates and nitrites, keytones, aldehydes, sulfuric acid, as well as explosive materials such as C4, Semtex, and ANFO's. Materials for which Raman is the only form of spectroscopic information includes water and non-aromatic amino acids, alcohols, and aliphatics. In Fig. 2, some materials, shown ringed in black below, strongly absorb both excitation and emission energy. These include active explosive ingredients, but also DNA and other compounds. However, even weakly fluorescent materials are still strong emitters compared to Raman.

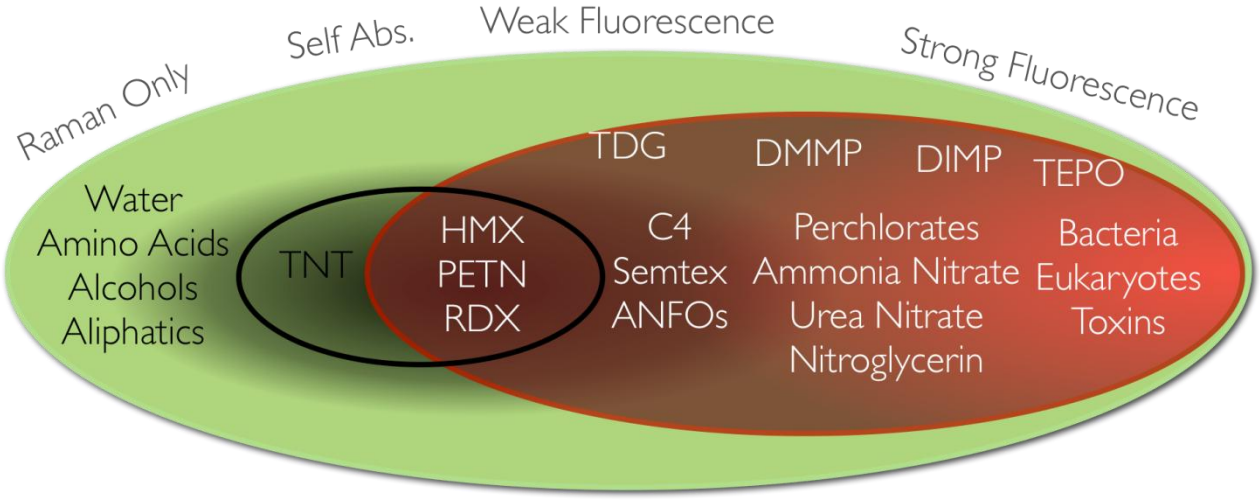

Figure 2. Overall relationship between the Raman and fluorescence information from weakly and strongly absorbing target material.

An additional advantage of using deep UV excitation is that because such a wide array of important target materials strongly absorb a these wavelengths, there is a natural spatial separation of superficial material from substrate or background material, which assists in discriminating the "topical" material from "deeper" material and provides a method of segregation of mixed materials.

4. DETECTION & DIFFERENTIATION WITH FLUORESCENCE ALONE

Figure 3 shows the fluorescence emission spectra of different compound and composite materials (such as bacterial spores and cells) with excitation at 224 nm, where the emission spectra of CH and OH Raman bands is shown along with the native fluorescence emission spectra of BTEX (benzene, toluene, ethylbenzene, and xylene), gasoline, diesel, bacteria, naphthalenes, explosives, proteins, and soot. Because the Rayleigh line is so intense, it has been eliminated along with the weaker Raman bands to put the Raman and native fluorescence emissions in proper perspective. Larger ring organics emit dominantly at longer wavelengths.

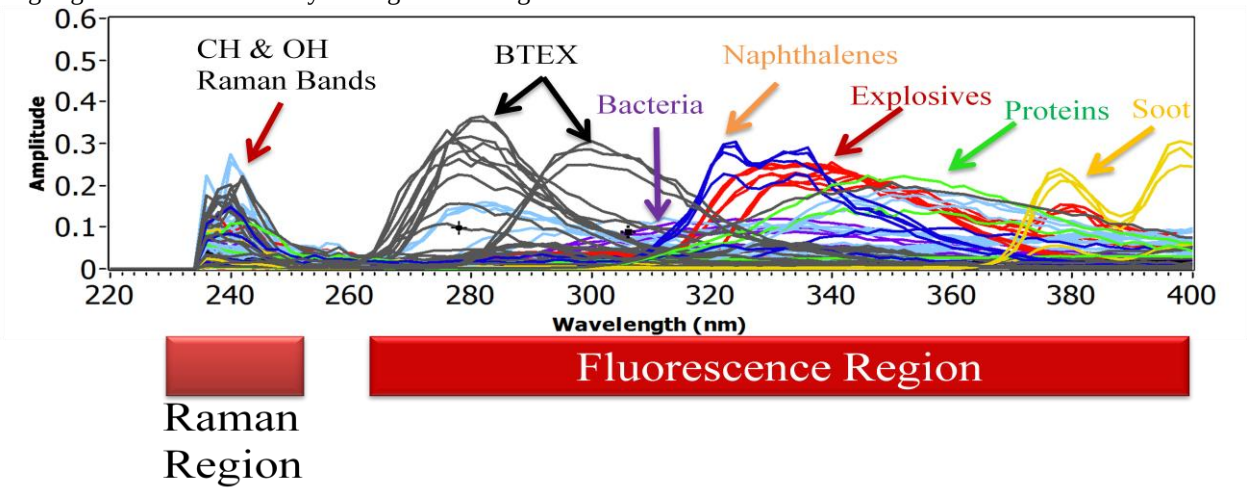

Figure 3. Separate Raman and native fluorescence emission spectra with excitation at 224 nm.

Excellent separation still occurs when excitation is at 248 nm. However, when laser excitation occurs at 263 nm or 266 nm, Raman spectra are obscured by native fluorescence from biological material, BTEX, and other simple organic materials at Raman shifts above 1000 cm-1 and 600 cm-1, respectively. Even the small excitation wavelength difference between 248 nm and 263 nm has been shown to completely mask Raman emissions from the most common "G" agents.

Detection of materials with any analytical method requires a database of samples against which an unknown sample can be compared. To understand the effect of a changing parameter, e.g. spectral resolution or spectral range, one needs to "visualize" changes in the relationship between samples as a parameter is varied. Multivariate analyses offer a solution by reducing the dimensionality of the input data; isolating components that provide the greatest separation. Using an approach like principal component analysis (PCA), samples that are spectrally alike, will cluster together. This alone is not sufficient and an expert must determine whether the materials in the groups are, in fact, related. For example, if one were to observe fluorescence from 270 nm to 400 nm, groups will have a first order separation based on their aromaticity (number and arrangement) and a second order effect that separates small aromatic compounds based on how they may be functionalized (-OH, -CH3, Cl, NH3, COOH, etc). However, when one decreases the observed spectral range to 270 - 350 nm, larger ring organics begin to "cluster" with small ring organics. Small fluorescence features in the lower wavelength region that do not account for the majority of the fluorescence begin to predominate when the longer wavelengths are ignored. This effectively "breaks" the chemometric analysis and relates chemicals that have little in common.

When chemical clustering occurs correctly, samples in one cluster should have some commonality where nearby clusters should consist of samples with minor variations associated to small changes in the chemistry (i.e., the second order separation). If these changes are small, e.g., benzene versus a spore (containing dityroine), these clusters should be closer than chemicals like benzene and anthracene (one ring versus 3 ring aromatics). In the case above, where aromaticity drives separation and a reduction in spectral range causes anthracene to closely cluster with benzene, these should never be nearby in chemometric space. In this case, the cluster containing anthracene can technically be a separate cluster. However, the gap between them limits the variations that may exist in nature and it is likely that a secondary effect that slightly alters the benzene fluorescence may appear in the anthracene cluster.

Figure 4 shows the PCA plot of 27 samples for which we have both Raman and fluorescence spectra. Excitation was a 248 nm using a NeCu laser. The circular arrow is a rough trend line beginning with samples that have strong UV fluorescence (Benzene) to samples that fluoresce in the blue (Anthracene). The primary factor, as expected, is the aromaticity of the samples with some influence of hetroatoms and side chains. These samples are not as well separated in PCA space as would be if excitation would have been at a wavelength at 224 nm or 235 nm [8]. However, as indicated, bacterial cells and spores, added for reference, are still separable and appear in a unique position in PCA space. In addition, explosive materials such as Semtex and PETN occupy a unique position in this PCA space. Acetone, a component of TATP, also fits this latter category. The fluorescence feature of acetone was unexpected in that no aromatic ring exists however it has been shown in the literature that this feature, which consists of both fluorescence and phosphorescence effects, applies to similar small ketones. Another sample, labeled as Mellitic, appears between the strong Benzene and Anthracene groups. Its placement in PCA chemometric space occurs since the spectral response of this sample has features of both groups (see Fig. 7). It is likely that the higher wavelength fluorescence comes is a result of phosphorescence.

This latter aspect regarding phosphorescence appears to be playing a larger role than previously expected. The samples that have been highlighted in Red circles and labeled M, S, and G are MES [2-(N-morpholino) ethanesulfonic acid], serine and glycine. The emission from MES could be attributed to the sulfonic group. O=S=O has a fluorescence feature and has been previously shown in the literature (Brus L.E and McDonald J.R, Chem Phys Let. 1973, vol 21, 2, p283). Whether the morpholine group shifts the O=S=O spectrum or if it is phosphorescence is not clear at the moment. However based on the prior studies on phosphorescence of serine and glycine, we attribute the signatures seen for these two samples as phosphorescence.

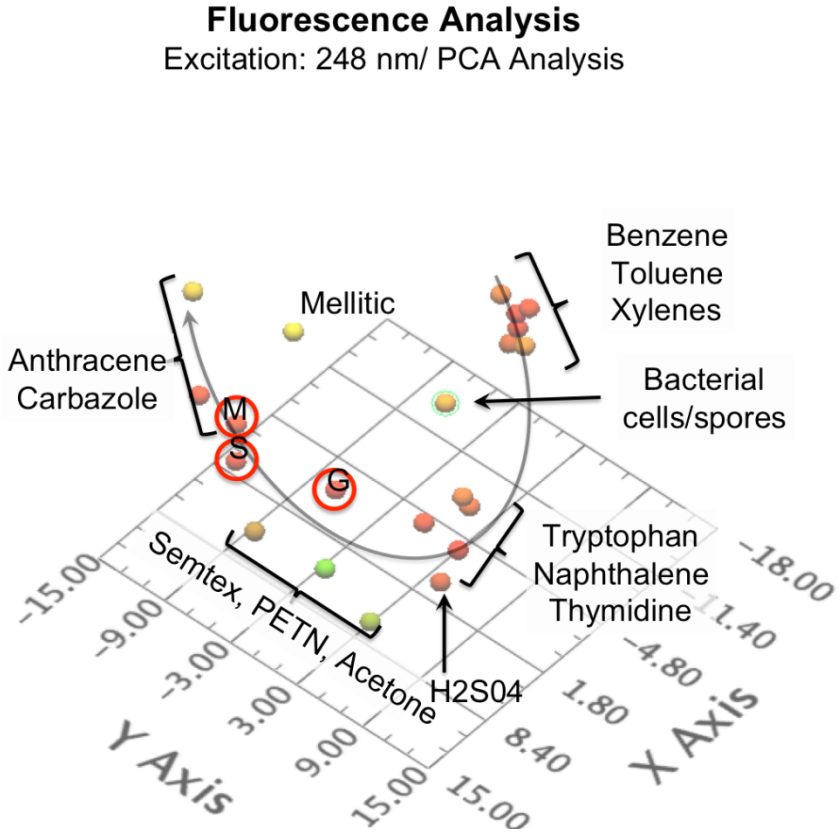

Figure 4. Fluorescence analysis of the 27 samples in the 248 fluorescence Raman database.

Another attribute to note is the native fluorescence feature of H2S04 (sulfuric acid) (shown in Fig. 4). This matches to the S02 fluorescence described in Brus and McDonald publication with excitation at 290 nm. However no reference to H2SO4 fluorescence has been found. It is not clear whether this is some sort of aromatic contamination however given the intensity of the response, it is likely intrinsic to the samples. The H2SO4 "fluorescence" correlates most closely to the naphthalene or tryptophan fluorescence.

5. DETECTION & DIFFERENTIATION WITH RAMAN ALONE

A similar PCA process can be applied to Raman data. All the following data were taken using the same 248 nm NeCu laser. The data preprocessing was limited to setting the spectral range, matching of spectral resolution, smoothing and normalization of each data type. To do this, a custom Labview program was written. Spectral ranges for the Raman spectra were set 750 – 3050cm-1 and the fluorescence range was set as 275 – 450 nm. The Raman range was truncated below the water Raman band (centered at ~3400cm-1. Therefore, for these data, the O-H stretching mode at 3400 cm-1 was not included in the analysis. The PCA plots that follow are 3D plots. To provide some dimensionality in the Z-dimension (PC-3), a color ramp was used. In all cases green/brown points are low (negative) Z-values, yellow are high (positive) Z-values, and red/orange are Z-values near zero.

Figure 5 shows a PCA analysis using only the Raman spectra associated to each of the 27 samples in the fluorescence/Raman database. Unlike the fluorescence analysis, which separated based on stokes shift (electronic transitions), the Raman spectra are clustered in groups with similar functional groups. Three main "groups" are present and have been identified with red, yellow and green circles. The red circle encompasses samples that are dominated by aromatic structures and contain the 1600 cm-1 features of C=C vibrations. The yellow circle encompasses the amino acids that are separated by the presence of the 2500-2800 cm-1 features associated to NH2 oscillations and the 1409 cm-1 -COO sym stretch. The third group is encompassed in a green circle. These samples group since they all are dominated by the C-H stretching modes. It so happens that many of these are alcohols and if the OH stretch were included, these samples would still group together. One sample in this green group, the simple ketone acetone, has an additional C=O feature that causes some slight separation from the other members of the group.

In addition to these groups, there are other samples that fall in-between or do not have sufficient number of samples to form a group. Samples like 1,2 dichloroethane (circled with green and purple) have functional groups that associate to samples exhibiting a C-H stretching mode, but also contains a C-Cl bond that appear to result in a weak 1250cm-1 band. The sample of toluene circled both red and green, also has two distinct features, an aromatic (1600cm-1 feature) and a strong C-H stretch.

The H2S04 sample creates a unique spectral features at 905, 1033, and 1153 cm-1 associated to the O=S=O vibrations. Some of these features are also seen the MES sample. However since MES also exhibits N-H bond oscillations, it exists between H2SO4 and the amino acids.

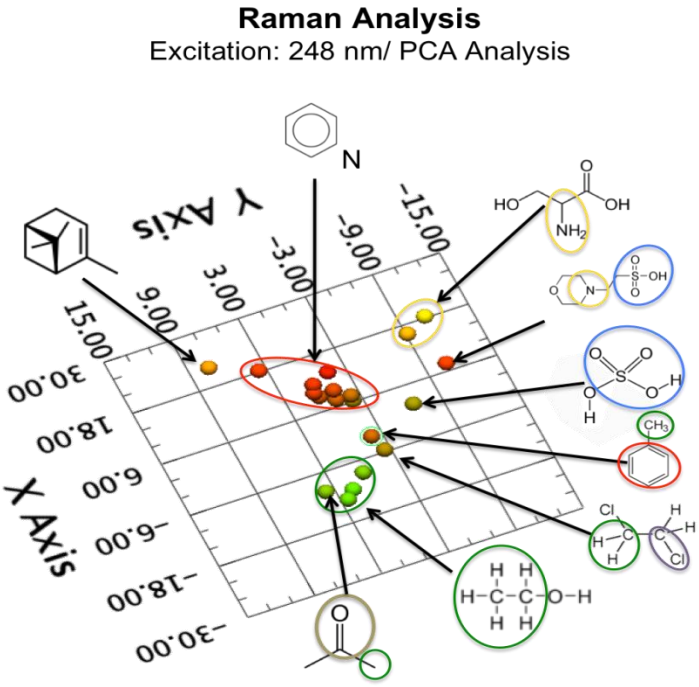

Figure 5. Raman analysis of the 27 samples in the 248 fluorescence Raman database.

The final sample that is separated from the aromatic samples is turpentine. This sample is a mixture but consists primarily of alpha-pinene (pictured). This sample has a very strong 1600cm-1 band but not the 1370cm-1 band that many of the aromatic have. Although there are C-H stretching modes, their influence on the placement of this compound PCA is space is minimal.

Samples of explosives (Semtex) or components of explosives (RDX or PETN) were not included in this dataset. As described above, the Raman spectra that we currently have (courtesy of Gaft) appear to be "burnt". When placed into the dataset they cluster together but since the D-G graphitic bands dominate their signatures, they were removed from this set and the combined dataset.

The PCA plot of the Raman data can be re-annotated to show the trends described above. This can be seen in Fig. 6. This method of describing the PCA plot will be used for the Raman/fluorescence

fusion data below. The direction of the arrow point towards samples whose chemometric positions are being dominated by the band(s) indicated.

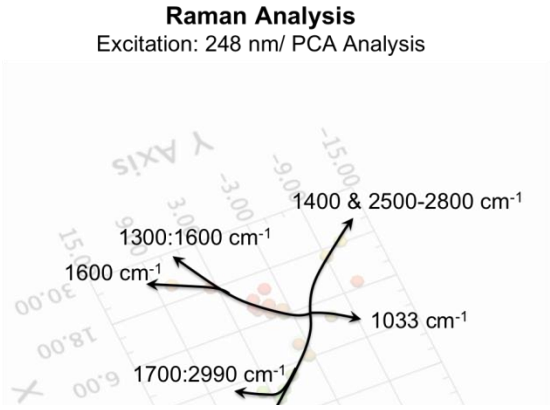

Figure 6. Raman trend analysis of the 27 samples in the 248 fluorescence Raman database.

Given either the fluorescence or Raman data, there are samples that can results in false classifications. In some cases, like the aromatic cluster in the Raman data, the separation between samples with a group rely on such small variations that it is likely that trace samples would result in incorrect results. Using a two step method of analysis, a sample, say a bacterial sample, would likely fall within the aromatic group of the Raman data (since it is has strong 1300 and 1600 cm-1 bands – Fig. 6.). However if the bacterial sample and the aromatic group to which it correlates are processed using the fluorescence data, the bacterial signature would uniquely separate (see Fig. 7).

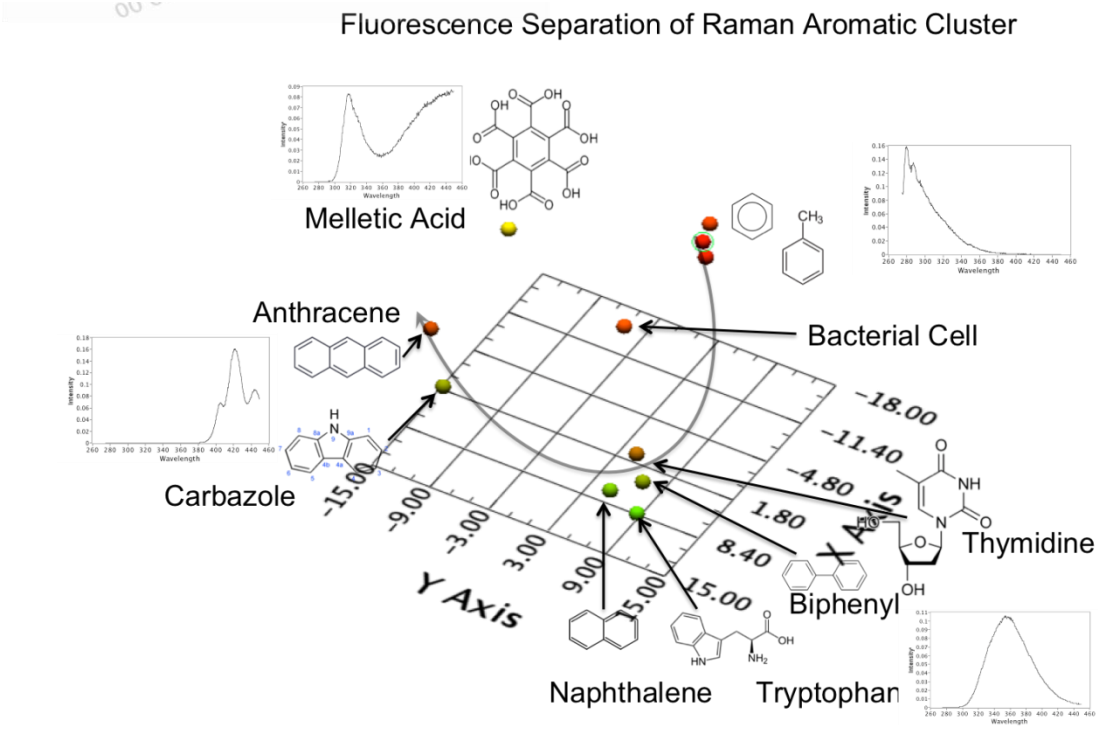

Figure 7. A two step analysis that uses fluorescence to elucidate samples within the aromatic cluster of the Raman analysis.

6. DETECTION & DIFFERENTIATION WITH FUSED RAMAN & FLUORESCENCE

The data described above show the capabilities of fluorescence or Raman used separately. To reiterate, fluorescence separated by the aromaticity of the samples where heteroatoms such as nitrogen or electronegative side groups may cause some spectral shifting that can be detected. Raman on the other hand separates by the presence of key vibrational bands such as C=C, C=O, CH, NH, S=O, etc.

For each samples we combined its fluorescence and Raman data using a custom labview program and ran a PCA analysis on the combined dataset. The results show that both the Raman and fluorescence data are causing separation of the samples. This is the first reported result of fusion analysis for deep UV fluorescence and Raman data to date.

In Fig. 8, the trendlines indicate how the samples are separated. The blue line is the effect of the fluorescence information and sets the "backbone" of the chemometric space. The 1400 to 1600 cm-1 Raman trendline closely follows this but causes some of the aromatic samples like turpentine to migrate away from the fluorescence trendline. The combination of low wavelength fluorescence and strong C-H stretching mode uniquely place toluene in the chemometric space. Xylenes however did not exhibit this C-H feature in its Raman spectrum. Therefore it clusters in the single ring group.

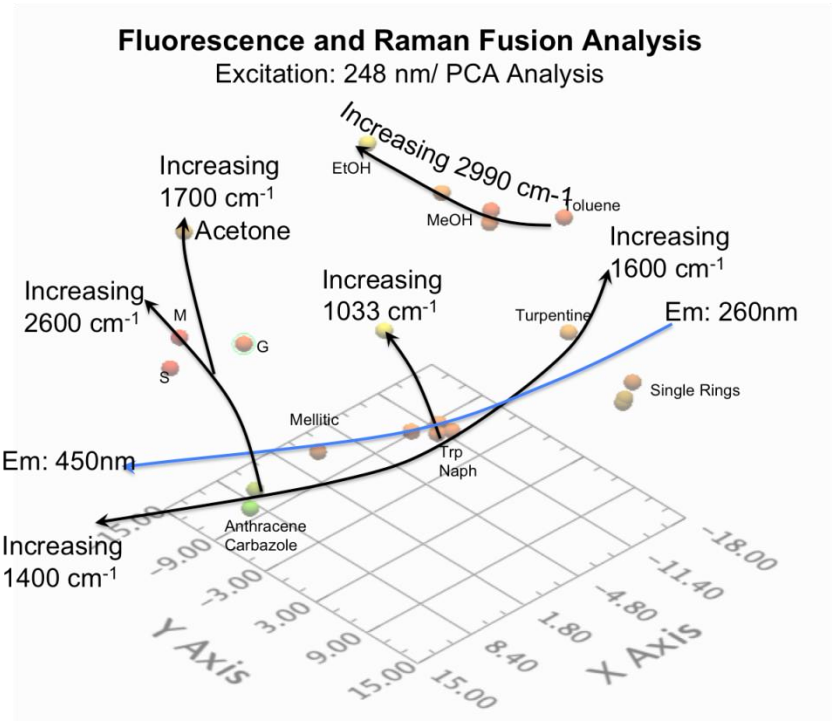

Figure 8. PCA analysis of fused fluorescence and Raman data with excitation at 248 nm.

The group that contains tryptophan, naphthalene, thymidine, and biphenyl does not separate from one another. Both their Raman and fluorescence spectra cause them cluster in a similar manner. This leads us to the conclusion that although there is enhanced detection and specificity, even the fused methods have limitations and will rely on 2 step methods described above.

Figure 9 below shows the same set of data but indicates which functional groups are causing the separation.

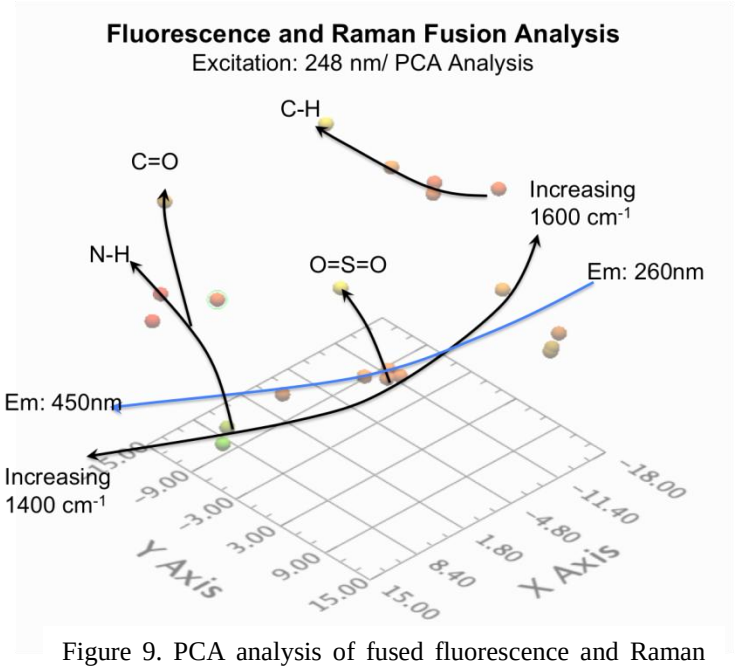

Figure 9. PCA analysis of fused fluorescence and Raman data with excitation at 248 nm.

1. ACKNOWLEDGEMENTS

Photon Systems gratefully acknowledges the support of this present effort under a U.S. Army STTR Contract No. W911SR-11-C-0089 under the program management of Dr. Augustus W. Fountain, and Dr. Steven Christesen.

2. REFERENCES

[1] Frosch, T., et.al. UV Raman Imaging, A promising tool. Anal. Chem. Vol.79, No.3, (Feb. 1, 2007)

[2] Asher, S.A., and C.R. Johnson, "Raman Spectroscopy of a Coal Liquid Shows That Fluorescence Interference Is Minimized with Ultraviolet Excitation", Science, 225, 311-313, 20 July (1984).

[3] Asher, S.A. and C.R. Johnson, "UV Resonance Raman Excitation Profile Through the $^1B_2$ State of Benzene", J. Phys. Chem. Vol. 89, pp.

1375-1379 (1985).
[4] Nelson, W.H., R. Manoharan and J.F. Sperry, "UV Resonance Raman Studies of Bacteria", App. Spect. Reviews, 27 (1), pp67-124, (1992)
[5] Sparrow, M.C., J.F. Jackovitz, C.H. Munro, W.F. Hug, and S.A. Asher, "A New 224nm Hollow Cathode UV Laser Raman Spectrometer", App. Spect., Vol. 55, No. 1, Jan (2001).
[6] Wu, M., M.Ray, K.H.Fung, M.W. Ruckman, D. Harder, and A.J. Sedlacek, "Stand-off Detection of Chemicals by UV Raman Spectroscopy", App. Spect., Vol.54, No.6, pp. 800-806 (2000).
[7] Hug, W.F., R. Bhartia, A. Tsapin, A. Lane, P. Conrad, K. Sijapati, and R. D. Reid, "Water & surface contamination monitoring using deep UV laser induced native fluorescence and Raman spectroscopy", Proc. SPIE, Vol. 6378, Boston, MA. Oct. (2006).
[8] Hug, W.F., R.D. Reid, R.Bhartia, and A.L.Lane, "Status of Deep UV Lasers for UV Resonance Raman and Native Fluorescence CBE Sensors", Invited Speaker, Conference on Lasers and Electro-Optics, PhAST 2, May 10, 2007
[9] Bhartia, R., W.Hug, E.Salas, R.Reid, K.Sijapati, A.Tsapin, W.Abbey, P.Conrad, K.Nealson, and A. Lane. "Classification of Organic and Biological materials with Deep UV Excitation", *Applied Spectroscopy*, Vol. 62, No. 10, October 2008.